

**Investigation of Clinical Absorption, Distribution, Metabolism, and Excretion and
Pharmacokinetics of the HIV-1 Maturation Inhibitor GSK3640254 Using an Intravenous
Microtracer Combined With EnteroTracker for Biliary Sampling**

Bo Wen, Ying Zhang, Graeme C. Young, David Kenworthy, Adrian Pereira, Jill Pirhalla, Janine
Doyle, Bethany Jordon, Joyce Zhan, and Mark Johnson

*GSK, Collegeville, PA, USA (B.W., Y.Z., J.P., J.D., J.Z.) and GSK, Ware, UK (G.C.Y., D.K.) and
GSK, Stevenage, UK (A.P., B.J.) and ViiV Healthcare, Durham, NC, USA (M.J.)*

Suggested running head (limit 60 characters, including spaces): PK and ADME study of
HIV-1 maturation inhibitor GSK3640254

Correspondence to:

Bo Wen

GSK R&D

1250 S Collegeville Rd

Collegeville, PA, 19426

Phone: 610-917-7000

E-mail: bo.1.wen@gsk.com

Number of text pages: 21

Number of tables: 3

Number of figures: 7

Number of references: 28

Abstract word count: 250

Introduction word count: 740

Discussion word count: 1267

Nonstandard abbreviations:

ADME, absorption, distribution, metabolism, and excretion

AMS, accelerator mass spectrometry

AUC, area under the curve

AUC_{0-t}, area under the plasma concentration-time curve from time 0 to last quantifiable
concentration

AUC_{0-∞}, area under the plasma concentration time-curve from time 0 extrapolated to infinity

C_{\max} , maximum observed concentration

E_h , hepatic extraction ratio

F , bioavailability

F_{abs} , fraction absorbed

F_g , fraction of drug escaping gut metabolism

F_h , fraction of drug escaping first-pass hepatic clearance

HPLC, high-performance liquid chromatography

IV, intravenous

LC, liquid chromatography

LC-MS/MS, liquid chromatography with tandem mass spectrometry

LLQ, lower limit of quantification

LSC, liquid scintillation counting

ML, metabolite load

PK, pharmacokinetics

t_{\max} , time of C_{\max}

$t_{1/2}$, terminal phase half-life

UGT, uridine diphosphate glucuronosyltransferases

V_{ss} , volume of distribution at steady state

ABSTRACT

GSK3640254 is a next-generation maturation inhibitor in development for HIV-1 treatment, with pharmacokinetics (PK) supporting once-daily oral dosing in human. This open-label, non-randomized, 2-period clinical mass balance and excretion study was used to investigate the excretion balance, PK, and metabolism of GSK3640254. Five healthy men received a single intravenous microtracer of 100 μ g [14 C]GSK3640254 with a concomitant oral non-radiolabeled 200-mg tablet followed by an oral 85-mg dose of [14 C]GSK3640254 14 days later. Complementary methods, including intravenous microtracing and accelerator mass spectrometry, allowed characterization of several parameters, including fraction absorbed, fraction escaping gut metabolism, hepatic extraction ratio, and renal clearance. Intravenous PK of GSK3640254 were characterized by low plasma clearance (1.04 L/h), moderate terminal phase half-life (21.7 hours), and low volume of distribution at steady state (28.7 L). Orally dosed GSK3640254 was absorbed (fraction absorbed, 0.26), with a high fraction escaping gut metabolism (0.898) and a low hepatic extraction ratio (0.00544), all consistent with low in vitro intrinsic clearance in liver microsomes and hepatocytes. No major metabolites in human plasma required further qualification in animal studies. Both unchanged parent GSK3640254 and its oxidative and conjugative metabolites were excreted into bile, with GSK3640254 likely subject to further metabolism through enterohepatic recirculation. Renal elimination of GSK3640254 as the parent drug or its metabolites was negligible, with >94% of total recovery of oral dose and >99% of the recovered radioactivity in feces. Altogether, the data suggest that systemically available GSK3640254 was slowly eliminated almost entirely by hepatobiliary secretion, primarily as conjugative and oxidative metabolites.

SIGNIFICANCE STATEMENT

The combination of an intravenous ^{14}C microtracer with duodenal bile sampling using EnteroTracker in a human absorption, distribution, metabolism, and excretion study enabled derivation of absorption and first-pass parameters, including fraction absorbed, proportion escaping first-pass extraction through the gut wall and liver, hepatic extraction, and other conventional clinical pharmacokinetic parameters. This approach identified hepatic metabolism and biliary excretion as a major elimination pathway for absorbed drug, which would be overlooked based solely on analyses of plasma, urine, and fecal matrices.

Word count (limit 80): 80

INTRODUCTION

GSK3640254 ((R)-1-fluoromethyl-4-(17-((2-(1,1-dioxidothiomorpholino)ethyl)amino)-28-norlupa-2,20(29)-dienyl)-cyclohex-3-ene-1-carboxylic acid methanesulfonate) is a next-generation HIV-1 maturation inhibitor exhibiting pan-genotypic coverage of HIV-1 subtypes and polymorphic variants (Dicker et al., 2021) and is currently in phase IIb clinical development for HIV-1 treatment. Maturation is one of the last steps of the HIV-1 cycle wherein the mature structural Gag proteins are generated by viral protease-mediated cleavage (Wang et al., 2015). Maturation inhibitors specifically interfere with the protease-mediated processing of Gag, resulting in the release of HIV-1 particles that are immature and noninfectious.

Human absorption, distribution, metabolism, and excretion (referred to as ADME) studies quantitatively and comprehensively evaluate a drug's overall disposition and are required for new drug approval (Coppola et al., 2019). Data obtained from human ADME studies provide valuable information for confirming whether the toxicology species are relevant for assessing a drug's safety and for developing a cohesive clinical pharmacology strategy, including investigation of potential drug–drug interactions and special patient populations (eg, patients with hepatic or renal impairment).

Intravenous (IV) pharmacokinetics (PK) are important for the calculation of primary PK parameters, such as bioavailability, clearance, and volume of distribution, which are necessary for a complete understanding of a drug's absorption, distribution, and elimination (Denton et al., 2013; Harrell et al., 2019). In conventional IV PK studies, healthy participants typically receive separate single therapeutically relevant IV and extravascular doses in a 2-way crossover design; however, the therapeutic IV dose would require an IV toxicology package to support its use in clinical studies. To bridge the “translational gap” between preclinical research and clinical development, exploratory clinical studies are nowadays encouraged to include microdosing to evaluate subtherapeutic exposures of drug candidates in first-in-human studies. Regulatory

guidance approves ultra-low dose (≤ 100 μg) IV administration in humans, which allows for a substantially reduced toxicology package (International Conference on Harmonisation of Technical Requirements for Registration of Pharmaceuticals of Human Use, 2009). In the microdosing approach, a ^{14}C -isotope may be incorporated into a drug, which allows for the measurement of systemic exposure using technologies such as accelerator mass spectrometry (AMS) (Harrell et al., 2019). Using a so-called IV “microtracer” design, microdosing studies may include concomitant administration of the ^{14}C -labeled microdose with a therapeutically relevant, extravascular dose to define IV PK (Lappin, 2016). Herein, we utilize an approach that intravenously administers a ^{14}C -microtracer dose of GSK3640254 concomitantly with the therapeutically relevant oral tablet dose of GSK3640254 ($2 \times 100\text{-mg}$ tablets) that is under clinical development.

Biliary disposition is an integral part of the human ADME profile. Metabolites can be abundantly formed in the liver but may not circulate in plasma (Loi et al., 2013). In addition, fecal metabolites do not necessarily represent hepatic metabolism due to degradation and/or metabolism by gut microflora (Wilson and Nicholson, 2017). Similar to applications of Entero-test devices, which are no longer commercially available, the EnteroTracker device (EnteroTrack LLC, Aurora, CO, USA) can be used to noninvasively collect duodenal bile samples and investigate human biliary disposition in humans (Guiney et al., 2011). To evaluate biliary secretion of a parent drug and its metabolites, duodenal bile sampling is preferred to stool sampling for many reasons, including providing an improved bile-specific metabolic profile without the potential contribution of gut microflora to metabolism (Bloomer et al., 2013; Harrell et al., 2019). Herein, we report the first-time application of EnteroTracker devices in a human ADME study in which duodenal bile samples were noninvasively collected, enabling characterization of biliary disposition of GSK3640254 and its metabolites and evaluation of the potential of enterohepatic recirculation.

Human ADME studies that include an IV dose can be used to estimate the absolute bioavailability (F) and oral fraction absorbed (F_{abs}) (Raje et al., 2018; de Vries et al., 2019; Harrell et al., 2019; Podoll et al., 2019; Johne et al., 2020). In preclinical species, GSK3640254 had low to moderate oral bioavailability dosed either as a spray dried dispersion or mesylate salt suspension (unpublished observations). Despite low turnover in liver microsomes or hepatocytes, absorbed drug-related material was primarily eliminated by metabolism followed by biliary secretion (~13% of the administered dose) in bile duct–cannulated rats dosed orally with [^{14}C]GSK3640254 mesylate salt (unpublished observations). Investigation of both the IV and oral PK of GSK3640254 and that of drug-related material in humans enables contributions of F_{abs} from the gastrointestinal tract and first-pass hepatic extraction to systemic exposure to be quantified. The study discussed herein aimed to fully characterize and understand the human ADME and PK of [^{14}C]GSK3640254 following both IV and oral administration.

MATERIALS AND METHODS

GSK3640254 mesylate salt, [^{14}C]GSK3640254 mesylate salt, and [$^2\text{H}_4$ $^{13}\text{C}_2$ ^{15}N]GSK3640254 were supplied by Chemical Development, GSK Research and Development (Stevenage, UK). GSK3640254 mesylate salt oral tablets were supplied by GSK (Ware, UK). The solution for IV infusion was manufactured by GSK (Ware, UK) from a stock solution of [^{14}C]GSK3640254 (2.5 mg/mL) dissolved in 3% weight/volume β -cyclodextrin sulfobutylether (Captisol[®]) and diluted to a concentration of 11 $\mu\text{g/mL}$ with 0.9% weight/volume sodium chloride in sterile saline. All other solvents and reagents were of analytical grade and were purchased from commercial suppliers.

Study Objectives and Design

This was an open-label, single-center, non-randomized, 2-period, single-sequence crossover study evaluating the PK, mass balance, excretion, and metabolism of GSK3640254 in healthy men (ClinicalTrials.gov identifier: NCT04507321). This study consisted of a screening visit and 2 on-site treatment periods separated by a ≥ 13 -day washout period (Figure 1). In treatment period 1, participants received a single oral tablet 200-mg dose of GSK3640254 with a moderate-fat meal and a 1-hour IV microtracer infusion of 100 μg [^{14}C]GSK3640254 mesylate salt (~ 3.7 kBq; 100 nCi) 5 hours after the oral dose to coincide with the anticipated maximal systemic exposures from the oral tablet administration. In treatment period 2, participants received an oral suspension of 85 mg [^{14}C]GSK3640254 (~ 3.15 MBq; 85 μCi) with a moderate-fat meal. Participants were fasted overnight for ≥ 8 hours before study treatment initiation in both treatment periods. EnteroTracker capsules were supplied by EnteroTrack, LLC (Aurora, CO, USA) to collect duodenal bile samples. The chemical structure of GSK3640254 has been previously published (Dicker et al., 2021). The structure of [^{14}C]GSK3640254 indicating the position of radiolabel incorporation is shown in Figure 2.

The primary objectives were to assess the rate and extent of excretion and total recovery of radioactivity in urine and feces in treatment periods 1 and 2, to determine systemic concentrations of parent GSK3640254 and total drug-related radioactivity in treatment periods 1 and 2, and to calculate the absolute oral bioavailability of GSK3640254 when given with food. Secondary objectives were to evaluate the safety and tolerability of GSK3640254 after single IV or oral doses and to determine the blood-to-plasma ratio of [^{14}C]GSK3640254–related materials. Exploratory objectives were to characterize the metabolic profile of GSK3640254 in treatment periods 1 and 2 and to assess the PK and relative bioavailability of GSK3640254 after administration of an 85-mg oral suspension compared with 200-mg tablets (2 × 100-mg oral tablets).

The oral doses of GSK3640254 used in treatment periods 1 and 2 were within the projected therapeutic range for HIV-1 treatment (50-200 mg) based on modeling and simulation of virology and PK data as well as results from the phase IIa proof-of-concept study of GSK3640254 in HIV-1–positive adults (Spinner et al., 2022). A 100- μg [^{14}C]GSK3640254 microdose was selected for IV administration in treatment period 1 because GSK3640254 had not been previously administered via IV infusion in humans. The IV infusion was administered concomitantly with a 200-mg oral non-radiolabeled GSK3640254 dose to ensure that the IV PK could be defined at therapeutically relevant systemic exposures. For both treatment periods combined, the total estimated radiation exposure was <1 mSv, thereby complying with the International Commission on Radiological Protection's recommendation of a 1-mSv maximum for category IIa projects (0.1-1 mSv; minor risk) (International Commission on Radiological Protection, 1992).

This study was conducted at Hammersmith Medicines Research (London, UK) in accordance with the Declaration of Helsinki. The study protocol and conduct were approved by the London Brent Research Ethics Committee (London, UK). All participants provided written

informed consent. Safety assessments included vital sign measurement, routine laboratory tests, 12-lead electrocardiograms, and adverse event monitoring throughout the study.

Study Participants

Eligible participants were healthy men aged from 30 to 50 years with a body weight of ≥ 50 kg, a body mass index between 19 and 31 kg/m², and a history of regular bowel movements. Participants had no recent or chronic history of diarrhea, no history of drug abuse, no regular alcohol or tobacco use in the previous 6 months, no clinically relevant disease, and had not been exposed to significant radiation in the previous 3 years. Participants with use of over-the-counter or prescription medications, including analgesics, herbal medications, or grapefruit or Seville orange juices, within 14 days before study treatment until study completion were excluded. Full eligibility criteria can be found on ClinicalTrials.gov (NCT04507321; <https://clinicaltrials.gov/ct2/show/NCT04507321>).

Sample Collection and Processing

Blood samples were collected in dipotassium ethylenediaminetetraacetic acid tubes through 8 days after dosing in treatment periods 1 and 2, and plasma was separated via centrifugation. Urine and fecal samples were collected through 8 days after dosing in treatment periods 1 and 2, which was extended up to 15 days after dosing in participants for whom excretion took longer than anticipated in treatment period 2. Duodenal bile was collected using a non-invasive bile string EnteroTracker device (Guiney et al., 2011). Briefly, participants pulled the first 10 to 20 cm of nylon out from the EnteroTracker capsule by the protruding loop and held the loop outside of the mouth while the capsule was swallowed with up to 350 mL of water. The string was then securely attached to the participant's face with adhesive tape over the loop. In treatment period 1, the bile string was swallowed 2 hours after the oral dose and 3 hours

before the IV infusion started, a duration recommended to allow transit of the string to the duodenum. Participants fasted from insertion of the bile string until the completion of the IV infusion, at which point a food cue (small, standard, high-fat meal) was given to stimulate gallbladder emptying. The EnteroTracker was removed ~1.5 hours after the IV infusion stopped (~7.5 hr after the oral dose) to capture the bile samples. In treatment period 2, the EnteroTracker was swallowed 2 hours after the oral dose. At 5.5 hours after the oral dose, a food cue (small, standard, high-fat meal) was given to stimulate gallbladder emptying. The collection bile string was removed 1.5 hours after the food cue (~7 hrs after the oral dose) to capture the duodenal bile samples expelled from the gallbladder. Samples of urine, feces, and bile strings were stored frozen before shipment for analysis.

Sample Analysis

Mass balance and excretion

Total radioactivity excreted in urine and fecal samples was determined using liquid scintillation counting (LSC) or AMS in treatment period 1 (IV; Pharmaron, Inc., Germantown, MD, USA) and using LSC in treatment period 2 (oral; Labcorp Drug Development, Harrogate, UK; summarized in Supplemental Table 1). Accelerator mass spectrometry was used to analyze samples with radioactivity levels that were too low to be detected using LSC. Because LSC and AMS have been individually qualified in the literature (Garner et al., 2000; Keck et al., 2010), cross validation between techniques was not performed for this study. Procedures for urine and fecal sample preparation and measurement of radioactivity by LSC and AMS have been previously described and key methodology is summarized here (Harrell et al., 2019). Efficiency correlation curves for LSC were confirmed using ^{14}C quenched standards. For AMS, instrument standards and process standards for graphitization were analyzed. Radioactivity in urine samples was measured in triplicate by LSC using a Packard TriCarb liquid scintillation counter

(Canberra Packard, Pangbourne, Berkshire, UK). Fecal samples were combusted (PerkinElmer Sample Oxidizer; Pangbourne, Berkshire, UK), absorbed in Carbo-Sorb (PerkinElmer), and combined with PermaFluor E+ scintillation fluid (PerkinElmer). Oxidation efficiency was determined by combustion of quality control standards and had to be 95% to 105% at the beginning and end of each run to be acceptable. Values were not corrected for combustion efficiency. Lower limits of quantification (LLQs) were established as two times the mean of background disintegrations, with mean LLQ values of 0.01 ng GSK3640254 Eq/g in urine and 186 ng Eq/g in fecal samples.

After undergoing combustion (oxidation) and graphitization (reduction), total radioactivity levels in urine and fecal samples were determined by AMS using a Single Stage AMS 250KV system (National Electrostatics Corporation, Middleton, WI) (Young et al., 2008). Mean LLQ values were 8.99 pg GSK3640254 Eq/mL in urine and 84.6 pg Eq/g in fecal samples.

PK assessments

Plasma samples were analyzed for GSK3640254 concentrations by PPD (Middletown, WI, USA) using a validated analytical method based on protein precipitation followed by liquid chromatography (LC) with tandem mass spectrometry (LC-MS/MS), as previously described (summarized in Supplemental Table 1) (Pene Dumitrescu et al., 2021). The lower limit of quantification was 3 ng/mL using a 50- μ L aliquot of plasma, and the higher limit of quantification was 1000 ng/mL. Plasma total radioactivity was analyzed by Pharmaron, Inc. using AMS analysis, with lower limits of quantification of 48.4 pg GSK3640254 Eq/mL in treatment period 1 and 43.2 pg Eq/mL in treatment period 2. Plasma [14 C]GSK3640254 concentrations were analyzed by Pharmaron, Inc. using a validated analytical method based on protein precipitation followed by LC + AMS analysis. Using a 500- μ L aliquot of plasma, the lower limit of quantification was 60.9 pg/mL, and the higher limit of quantification was 1830 pg/mL.

The LC-MS/MS and LC + AMS analytical methods included quality control samples containing GSK3640254 and [^{14}C]GSK3640254 at 3 different concentrations, which were stored and analyzed all samples against calibration standards, which were separately prepared. For analyses to be acceptable, $\leq 33\%$ of quality control results and $\leq 50\%$ of results from each concentration level could deviate from the nominal concentration by $>15\%$ for LC-MS/MS and $>20\%$ for LC + AMS. Applicable analytical runs met all predefined run acceptance criteria.

Quantification and Characterization of Metabolites

Procedures for the quantification and characterizations of metabolites have been previously described and key methodology is summarized here (Harrell et al., 2019). The metabolic profile of plasma extracts from treatment period 2 (oral), homogenized fecal extracts from treatment period 1 (IV), and bile string extracts from both treatment periods were characterized by Pharmaron, Inc. using LC + AMS (summarized in Supplemental Table 1). Plasma samples from individual participants in treatment period 2 were pooled using an area-under-the-curve (AUC) approach (Hamilton et al., 1981; Hop et al., 1998) from time 0 to 24 and 0 to 96 hours and then further pooled across participants by combining volumes in proportion to the time interval between individual samples to prepare a single plasma pool. The 0- to 24-hour AUC pools were used to allow a direct comparison with those of nonclinical species, whereas plasma toxicokinetic and ^{14}C -metabolite profiles were determined over a 0- to 24-hour time period. Consequently, the 0- to 96-hour AUC pools were analyzed to capture the majority ($>90\%$) of ^{14}C radioactivity in human plasma samples. Homogenized fecal samples were pooled based on a ratio of the total weight of the sample excreted at each time point such that the pool represented $\geq 95\%$ of the total excreted ^{14}C across all participants. An equal weight of sample from each individual pool was obtained to prepare a combined fecal pool. Plasma and fecal samples were extracted with a 50:50 mixture of methanol to acetonitrile (volume/volume, 3-4.5

volumes) 2 times, dried under a stream of nitrogen gas, and reconstituted in a 10:10:80 mixture of dimethylsulfoxide to acetonitrile to water (volume/volume/volume). Bile strings were removed from the freezer and thawed at room temperature for as short a time as is practically possible. Each string was immediately placed inside the barrel of a hypodermic plastic syringe, and duodenal bile was extracted individually with high-performance LC (HPLC)–grade acetonitrile and then HPLC-grade water. The organic extracts from treatment period 1 (IV bile) were dried and then reconstituted with 250 μ L of 10-mM ammonium formate (pH = 4) in a 9:1 mixture of LC-grade water to HPLC-grade acetonitrile containing 0.1% formic acid (pH = 4; volume/volume), while the combined extracts from treatment period 2 (oral bile) were diluted 100-fold with 10 mM ammonium formate (pH = 4). Extracts were pooled from individual participants, and extracts containing radioactivity above LSC background were pooled across participants.

The metabolic profile of fecal samples from treatment period 2 (oral) was characterized by Q2 Solutions (Morrisville, NC, USA) using HPLC-MS/MS. Representative fecal samples containing >1% of the administered dose were pooled by total weight ratio to obtain a pool containing >95% of the radioactivity excreted in each participant. Fecal samples were extracted with a 50:50 mixture of methanol to acetonitrile, centrifuged evaporated under nitrogen, and reconstituted in a 1:1:8 (volume/volume/volume) mixture of dimethyl sulfoxide to acetonitrile to water. The amount of radioactivity in the extracts was determined by LSC before radio-HPLC analysis. Radio-HPLC data were captured off-line by collecting fractions into 96-well Scintiplates (PerkinElmer, Waltham, MA, USA). Each HPLC eluate was evaporated to dryness under centrifugal vacuum, the dried plates were sealed, and a microplate scintillation counter with 12 independent photomultiplier tubes was used to count each well; no background was subtracted.

Data analyses from AMS and scintillation counting data from off-line analyses were converted into a form compatible with Laura software (LabLogic Systems, Inc., Tampa, FL,

USA) using its “LSC import” function to reconstruct AMS and radio-HPLC radiochromatograms. The area in each radioactive peak was expressed as a percentage of the total number of counts detected.

Pharmacokinetics and Statistical Analyses

No formal sample size calculation was performed. A sample size of 4 to 6 participants was deemed appropriate to achieve the objectives of the study (Penner et al., 2009). This study used WinNonlin software version 6.3 or higher (Certara, Princeton, NJ, USA) to non-compartmentally analyze the parent drug following oral tablet or suspension administration and IV administration (plasma GSK3640254 and [^{14}C]GSK3640254, respectively) as well as total radioactivity concentration-time data based on actual recorded sampling times for derivation of PK parameters. Clearance, volume of distribution at steady state (V_{ss}), and oral bioavailability for each oral formulation (tablet or suspension) were calculated for GSK3640254 in plasma. Pharmacokinetic parameters for GSK3640254, [^{14}C]GSK3640254, and total radioactivity following IV infusion and oral administration were summarized descriptively. Absorption and first-pass PK parameters for GSK3640254, including fraction of drug escaping first-pass hepatic clearance (F_h), hepatic extraction ratio (E_h), fraction of drug escaping gut metabolism (F_g), and F_{abs} , were calculated as previously described (Harrell et al., 2019).

RESULTS

Study Population

Of the 17 individuals screened, 5 participants were enrolled and completed the study. One protocol deviation was reported for a participant who met exclusion criteria (past or intended use of over-the-counter or prescription medications); this participant was rescreened after meeting eligibility criteria and enrolled. All participants were men, with a mean age of 37 years and a mean body mass index of 24.8 kg/m² (Supplemental Table 2).

Mass Balance and Excretion

The mean recovery of radioactivity over time following IV and oral administration of [¹⁴C]GSK3640254 is shown in Figure 3. Following IV administration of [¹⁴C]GSK3640254, the majority of radioactivity was excreted within 96 hours (53% of dose) and a total of 76% of the administered dose was recovered within 7 days, with 74% of the dose being recovered in feces and <2% in the urine. Normalized for recovery, fecal excretion was predominant, accounting for 97.5% of the total recovered radioactivity, with ~2.5% in the urine (Figure 3A). Following oral administration of [¹⁴C]GSK3640254, 75% of the administered dose was recovered within 96 hours, and a total of >94% of the administered dose was recovered within 7 days. Similarly, excretion was predominately in the feces, accounting for >99% of the total recovered radioactivity (Figure 3B), with <0.6% of the administered dose recovered in the urine.

Pharmacokinetic Results

Following oral administration of GSK3640254 (2 × 100-mg tablets) in treatment period 1, the maximum observed concentration (C_{\max}) was reached with a median time of C_{\max} (t_{\max}) of 7 hours followed by a slow decline in concentrations, with a geometric mean terminal phase half-life ($t_{1/2}$) of 24.1 hours (Table 1; Figure 4A). The geometric mean F of GSK3640254 following

oral tablet administration was 21.4% (90% CI, 19.4% to 23.5%; Table 2) based on dose-normalized AUC from time 0 extrapolated to infinity ($AUC_{0-\infty}$) relative to the IV microtracer dose.

Following IV infusion administration of [^{14}C]GSK3640254 in treatment period 1, similar concentration-time profiles were demonstrated for both [^{14}C]GSK3640254 and total radioactivity, with C_{\max} occurring at the end of the 1-hour infusion (median t_{\max} = 0.983 hours; Table 1; Figure 4B). These data demonstrated that GSK3640254 is the predominant contributor of total radioactivity in plasma, with a minimal contribution of metabolite(s) to the drug-related material in systemic circulation. Plasma concentrations of [^{14}C]GSK3640254 steadily declined from C_{\max} with a geometric mean $t_{1/2}$ of 21.7 hours. The geometric mean plasma clearance of [^{14}C]GSK3640254 was low (1.04 L/h) and the geometric mean V_{ss} was low (28.7 L) and close to the volume for extracellular fluid, indicating that there is low distribution of the drug outside the systemic circulation. After correction of the plasma clearance with a human blood-to-plasma ratio of 0.5 (Table 1), the human blood clearance is 2.08 L/h (1.04 L/h/0.5), which is equal to 2% of liver blood flow relative to a human hepatic blood flow of 87 L/h (Davies and Morris, 1993). The geometric mean renal clearance was 0.02 L/h, providing a negligible contribution to the overall total clearance. Following IV infusion, ratios of plasma concentrations of [^{14}C]GSK3640254 to total radioactivity demonstrated that GSK3640254 is the predominant contributor to total radioactivity in plasma (Supplemental Table 3).

Following oral administration of [^{14}C]GSK3640254 as an 85-mg oral suspension, [^{14}C]GSK3640254 and total radioactivity had similar plasma concentration-time profiles, reaching C_{\max} with a median t_{\max} of 4 hours and slowly declining thereafter (Table 1 Figure 4C). The geometric mean $t_{1/2}$ of [^{14}C]GSK3640254 was 24.2 hours. Using total radioactivity in urine as a surrogate for GSK3640254 urine concentration, the calculated oral renal clearance was low (0.01 L/h). Following oral suspension administration of [^{14}C]GSK3640254, the geometric mean C_{\max} and AUC ratios of GSK3640254 for total radioactivity demonstrated that GSK3640254

accounts for ~82% to 93% of the total radioactivity in plasma (Supplemental Table 3). Systemic exposures of total radioactivity in blood were reduced compared with those for total radioactivity in plasma, with mean blood-to-plasma ratios of 0.480 to 0.595 up to 10 hours post-dose. Dose-normalized C_{\max} , $AUC_{0-\infty}$, and AUC from time 0 to last quantifiable concentration (AUC_{0-t}) were used to compare the relative bioavailability of the 85-mg oral suspension (treatment period 2) vs the 200-mg oral tablets (treatment period 1). The geometric mean AUC ratios of GSK3640254 exposures were close to 100% and 90% CIs for overall exposure (AUC_{0-t} and $AUC_{0-\infty}$) were within the Food and Drug Administration bioequivalence limit (0.80-1.25), suggesting that the 2 formulations were bioequivalent. The relative bioavailability of the oral suspension vs the oral tablet was slightly increased by 14% based on the C_{\max} and the 90% CI (0.992-1.32; Table 2).

Absorption and First-pass Pharmacokinetic Parameters

Geometric mean absorption parameters of GSK3640254 are presented in Table 3. The plasma metabolite load (ML; exposure ratio of metabolites to total radioactivity) following IV and oral delivery was low (0.0438 and 0.180, respectively). Following oral suspension administration, it is estimated that ~26% of GSK3640254 is absorbed (F_{abs}) across the gastrointestinal tract and only ~0.5% of the absorbed drug is cleared (E_h) before reaching the systemic circulation. Minimal loss of GSK3640254 was likely due to high fractions of drug escaping metabolism in the gut wall and liver, with an F_g value of 89.8% and an F_h value of 99.5%, respectively.

Metabolism

A putative metabolic scheme for GSK3640254 is shown in Figure 2. Accelerator mass spectrometry analysis of time-resolved pooled plasma extracts (0-24 hours and 0-96 hours) from oral dosed participants (treatment period 2) showed that GSK3640254 was the

predominant circulating component (87.4% and 85.0% of plasma radioactivity, respectively; Figure 5). The other notable radiolabeled components were identified as M4 (oxidation) and co-eluting M1 (acyl glucuronide conjugate) and M9 (N-dealkylation), accounting for 3.2% and 2.4% of the radioactivity in the pooled plasma (0-96 hours), respectively. Due to closely aligned total circulating radioactivity with the levels of circulating concentrations of GSK3640254, metabolite profiling was not performed in plasma samples from IV-dosed participants in treatment period 1. Representative AMS chromatograms of reconstituted pooled plasma extractions in treatment period 2 are shown in Figure 5.

Following IV infusion in treatment period 1, unchanged GSK3640254 was the predominant radioactive component in pooled fecal samples, accounting for 44% of total radioactivity and 32% of the dose; other notable radioactive components included M4 (oxidation; 7% of radioactivity), M8 (di-oxidation; 3.6% of radioactivity), and M9 (N-dealkylation) plus M28 (oxidation; labeled as "Unknown" and accounted for 9.0% of combined radioactivity; Figure 6A). All other radioactive components accounted for <4% of the total radioactivity. In pooled bile extracts following IV infusion, M1 (formed by acyl glucuronidation) was the major radioactive component, representing 41% of total radioactivity; other radioactive components included unchanged GSK3640254 (15% of radioactivity), M4 (oxidation; 11% of radioactivity), and M8 (di-oxidation; 6% of radioactivity; Figure 6B). All other radioactive components individually accounted for <4% of the total radioactivity.

Following oral administration in treatment period 2, the principal radioactive component in feces was unchanged GSK3640254, representing 84% of total radioactivity and 79% of the dose (Figure 7A). Other notable radioactive components included M4 (oxidation; 3% of radioactivity) and M9 co-eluting with M28 (5% of radioactivity; formed by N-dealkylation and oxidation, respectively). The remaining lesser radioactive components included M5 (oxidation), M7 (hydration), M8 (di-oxidation), M13 (hydration and oxidation), M14 (oxidation and N-

dealkylation), M18 (oxidation), M27 (oxidation), and M29 (oxidation and N-dealkylation), each <2% of radioactivity (Supplemental Table 4). Unchanged GSK3640254 also accounted for the majority of total radioactivity in pooled bile extracts following oral administration (94%), with other radioactive components each accounting for <1% of total radioactivity (Figure 7B); however, comparison of biliary metabolite profiles from IV- and oral-dosed participants suggested that GSK3640254 in bile samples from treatment period 2 comprised of primarily the unabsorbed GSK3640254. With the high radioactive dose in treatment period 2, it is likely that any potential contamination from the unabsorbed radioactive oral dose had significant impact on the metabolic profiles from oral-dosed participants.

Safety

No deaths, serious AEs, or AEs leading to study withdrawal were reported. Overall, 1 (20%) participant reported 3 AEs during the study. This participant reported AEs of asthenia and nausea that were mild in intensity during treatment period 1 and an additional AE of asthenia that was moderate in intensity during treatment period 2. All AEs were considered to be drug related and resolved within 2 days of onset. No clinically significant findings were reported for chemistry or hematology values, electrocardiographic parameters, or vital signs.

DISCUSSION

A combination of a ^{14}C IV microtracer and non-invasive EnteroTracker bile sampling techniques were used to fully characterize the ADME and PK of GSK3640254 in healthy men, with comprehensive information obtained for mass balance and excretion data, GSK3640254 and total radioactivity in plasma, and metabolite profiles in multiple matrices. This approach allowed for the derivation of absorption and first-pass parameters that are not typically reported in conventional clinical PK studies, including parameters such as F_{abs} , F_{g} , E_{h} , and geometric mean renal clearance. Incorporating a ^{14}C -isotope into the parent GSK3640254 molecule enabled human metabolism to be fully evaluated in both plasma and excreta, allowing for the assessment of exposure to circulating metabolites as well as the identification of elimination pathways. To ensure pharmacological relevance, the IV microtracer dose was concomitantly administered with a therapeutically relevant GSK3640254 oral dose ($2 \times 100\text{-mg}$ tablets), which is currently under clinical development. The first-time application of the non-invasive bile sampling via EnteroTracker devices enabled the assessment of biliary disposition of GSK3640254 and its metabolites. Most importantly, hepatic metabolism and biliary excretion were identified as a major elimination pathway for absorbed GSK3640254, which would otherwise be overlooked based solely on analysis of plasma, urine, and fecal matrices.

The total recovery of radioactivity achieved following oral suspension administration of 85 mg [^{14}C]GSK3640254 (3.15 MBq radioactivity) with food was 94%, which is in line with expectations for an acceptable mass balance recovery as established by the European Medicines Agency (European Medicines Agency, 2012). Although recovery of radioactivity was lower (76%) following IV infusion, it was only slightly below the 80% recovery threshold reported in a retrospective analysis of other mass balance clinical studies (Roffey et al., 2007). It is noteworthy to mention that the much lower radioactive microtracer dose (3.7 kBq) delivered by IV infusion did not permit recovery to be used for release criteria due to the slow data

turnaround; thus, a fixed collection period of 7 days after dosing was established in the study protocol. Excretion of GSK3640254 predominately occurred through the feces, accounting for 97.5% and >99% of total recovered radioactivity following IV and oral administration, respectively. By contrast, urinary excretion was minimal after administration of [^{14}C]GSK3640254 as an IV infusion (~2.5%) or oral suspension (<1%). Due to negligible radioactivity excreted in urine, no metabolite investigation was conducted in this matrix.

Intravenous administration of [^{14}C]GSK3640254 resulted in plasma concentration-time profiles characterized by low clearance and low V_{ss} . GSK3640254 exhibited blood clearance equal to 2% of human liver blood flow, and the V_{ss} (28.7 L) was less than the previously reported value for total body water (42 L) (Davies and Morris, 1993); these results suggest that limited distribution of GSK3640254 occurred outside of the plasma. Regardless of formulations, oral administration of GSK3640254 demonstrated good dose proportionality between the 200-mg oral tablets and 85-mg oral suspension. Following oral suspension administration, it is estimated that ~26% of dose is absorbed (F_{abs}) across the gastrointestinal tract. Although the oral F_{abs} was low, any absorbed GSK3640254 is likely subject to poor 'first-pass' metabolism by the gut wall ($F_g = 0.898$) and liver ($E_h = 0.005$; $F_h = 0.995$). Thus, it is postulated that the relatively low oral F (21.4%) was primarily driven by the low oral absorption rates rather than metabolic clearance or 'first-pass' effects. Key factors driving oral F can be better understood by dissecting oral absorption into specific parameters, such as absorption rate and gut and hepatic extraction (Harrell et al., 2019). Determining the 'first-pass' drug burden to the gastrointestinal tract and liver may also improve the evaluation of potential drug-drug interactions using physiologically based PK models. In addition, the low E_h and poor 'first-pass' effects of GSK3640254 in human are in parallel with the observed low intrinsic clearance in vitro in incubations with human liver microsomes and hepatocytes (unpublished observations). Despite the low F_{abs} , the minimal 'first-pass' effect and low clearance ensures delivery of adequate

exposures of GSK3640254 reaching the systemic circulation. The geometric mean elimination $t_{1/2}$ values were similar, ranging from 22 to 24 hours following administration as oral tablets, IV infusion, or oral suspension, suggesting that the rate of terminal elimination was not affected by the administration route (IV or oral). Based on geometric mean plasma [^{14}C]GSK3640254-to-total radioactivity ratios for C_{max} and AUC, unchanged GSK3640254 was the predominant contributor of total radioactivity in plasma following both IV infusion (>90%) and oral administration (82% to 93%).

The predominant circulating drug-related component in plasma was unchanged GSK3640254 after oral dosing. Several minor radioactive peaks representing ~2% to 3% of sample radioactivity were composed of 3 metabolites formed by acyl-glucuronidation, oxidation, and N-dealkylation. Therefore, no individual metabolite exceeded the 10% threshold of the total drug-related exposure outlined by the International Conference on Harmonisation and US Food and Drug Administration (International Conference on Harmonisation of Technical Requirements for Registration of Pharmaceuticals of Human Use, 2009; US Food and Drug Administration, 2020), above which further nonclinical evaluation may be justified. The metabolites identified in human plasma had chemical structures that were formed via common oxidative and conjugative routes and are considered as innocuous and unlikely to be reactive. Therefore, no human GSK3640254 metabolites need further evaluation in nonclinical studies. In addition, the levels of circulating radioactivity were closely aligned with the levels of circulating concentrations of GSK3640254, suggesting minimal levels of metabolites in plasma from the IV administration of [^{14}C]GSK3640254.

The acyl glucuronide M1 was a major component (41%) in human duodenal bile following IV administration but was not detected in fecal extracts (Figure 6), suggesting a rapid hydrolysis of the acyl glucuronide metabolite by the gut microflora. This likely contributed to a potential enterohepatic recirculation of GSK3640254, which may explain small fluctuations

(secondary uplifts) observed in the plasma PK profiles. Although only “snapshot” measurements, LC + AMS analysis of bile string extracts suggested that acyl glucuronidation (as M1) was a likely major route of elimination pathway of GSK3640254. Given that no or only trace levels of M1 were detected in other biological matrices, including plasma and feces, it is of importance that duodenal bile sampling bridges the gap in understanding the major elimination pathways of GSK3640254 in human. Based on in vitro phenotyping experiments, several uridine diphosphate glucuronosyltransferases (UGT) isoforms, including UGT1A4 and UGT2B7, were involved in glucuronidation of GSK3640254, with less contribution from UGT1A9 (unpublished observations).

It remains challenging to predict which metabolites formed in the liver will eventually circulate in plasma (Loi et al., 2013). Despite extensive hepatic metabolism observed in duodenal bile, unchanged parent GSK3640254 is the predominant circulating component in human plasma, with only trace levels of metabolites observed (Figure 5). This is in parallel with the low plasma ML (ratio of metabolite to total radioactivity) following IV (ML = 0.0438) and oral (ML = 0.18) administration (Table 3). Routes of metabolism included various oxidations, including acyl glucuronidation, N-dealkylation, mono- and di-oxidations, and combinations thereof. Apart from UGT-mediated conjugation reactions, cytochrome P450 3A4 was identified as the only cytochrome P450 isoform metabolizing GSK3640254 in incubations with human liver microsomes (unpublished observations). Overall, these data suggest that once absorbed, the systemically available GSK3640254 was eliminated primarily by hepatobiliary secretion in the form of metabolites. A high proportion of metabolic elimination is likely to result from acyl glucuronidation. Renal clearance is a negligible route of elimination.

In conclusion, this small, 2-part study using concomitant administration of IV and oral doses, state-of-the-art analytical technology, and thorough evaluation of ADME and PK parameters has rigorously characterized GSK3640254 disposition in human. These findings

subsequently helped the development of a cohesive strategy for clinical pharmacology studies, including drug-drug interactions and study of special patient populations.

ACKNOWLEDGMENTS

The authors would like to acknowledge the contributions of Mark Bush, Samit Joshi, and Martin Gartland for clinical study design and data interpretation, Jessica Shoultz and Yijun Yi (Q2 Solutions, Indianapolis, IN, USA) for conducting the LC-MS/MS metabolite identification work, Stephen English (Pharmaron, Inc., Germantown, MD, USA) for contributing to the AMS and LC + AMS analyses, and Lee Crossman (Labcorp Drug Development, Harrogate, UK) for contributing to the human excretion and mass balance analyses. Editorial assistance was provided under the direction of the authors by Megan Schmidt, PhD, and Lauren Bragg, ELS, MedThink SciCom, and was funded by ViiV Healthcare.

AUTHORSHIP CONTRIBUTIONS

Participated in research design: Wen, Zhang, Young, Kenworthy, Pereira, Pirhalla, Jordon, Zhan, Johnson

Conducted experiments: Pirhalla, Doyle

Contributed new reagents or analytic tools: Young, Kenworthy, Pereira

Performed data analysis: Wen, Zhang, Pereira, Pirhalla, Doyle, Zhan

Wrote or contributed to the writing of the manuscript: Wen, Zhang, Young, Kenworthy, Pereira, Pirhalla, Doyle, Jordon, Zhan, Johnson

REFERENCES

- Bloomer JC, Nash M, Webb A, Miller BE, Lazaar AL, Beaumont C, and Guiney WJ (2013) Assessment of potential drug interactions by characterization of human drug metabolism pathways using non-invasive bile sampling. *Br J Clin Pharmacol* 75: 488-496.
- Coppola P, Andersson A, and Cole S (2019) The importance of the human mass balance study in regulatory submissions. *CPT Pharmacometrics Syst Pharmacol* 8: 792-804.
- Davies B and Morris T (1993) Physiological parameters in laboratory animals and humans. *Pharm Res* 10: 1093-1095.
- de Vries R, Jacobs F, Mannens G, Snoeys J, Cuyckens F, Chien C, and Ward P (2019) Apalutamide absorption, metabolism, and excretion in healthy men, and enzyme reaction in human hepatocytes. *Drug Metab Dispos* 47: 453-464.
- Denton CL, Minthorn E, Carson SW, Young GC, Richards-Peterson LE, Botbyl J, Han C, Morrison RA, Blackman SC, and Ouellet D (2013) Concomitant oral and intravenous pharmacokinetics of dabrafenib, a BRAF inhibitor, in patients with BRAF V600 mutation-positive solid tumors. *J Clin Pharmacol* 53: 955-961.
- Dicker I, Jeffrey JL, Protack T, Lin Z, Cockett M, Chen Y, Sit SY, Gartland M, Meanwell NA, Regueiro-Ren A, Drexler D, Cantone J, McAuliffe B, and Krystal M (2021) GSK3640254 is a novel HIV-1 maturation inhibitor with an optimized virology profile. *Antimicrob Agents Chemother* Aac0187621.
- European Medicines Agency (2012) Guideline on the investigation of drug interactions. CPMP/EWP/560/95/Rev. 1 Corr. 2**. <https://www.ema.europa.eu/en/investigation-drug-interactions>. Accessed December 20, 2021.
- Garner RC, Barker J, Flavell C, Garner JV, Whattam M, Young GC, Cussans N, Jezequel S, and Leong D (2000) A validation study comparing accelerator MS and liquid scintillation

- counting for analysis of ^{14}C -labelled drugs in plasma, urine and faecal extracts. *J Pharm Biomed Anal* 24: 197-209.
- Guiney WJ, Beaumont C, Thomas SR, Robertson DC, McHugh SM, Koch A, and Richards D (2011) Use of Entero-Test, a simple approach for non-invasive clinical evaluation of the biliary disposition of drugs. *Br J Clin Pharmacol* 72: 133-142.
- Hamilton RA, Garnett WR, and Kline BJ (1981) Determination of mean valproic acid serum level by assay of a single pooled sample. *Clin Pharmacol Ther* 29: 408-413.
- Harrell AW, Wilson R, Man YL, Riddell K, Jarvis E, Young G, Chambers R, Crossman L, Georgiou A, Pereira A, Kenworthy D, Beaumont C, Marotti M, Wilkes D, Hessel EM, and Fahy WA (2019) An innovative approach to characterize clinical ADME and pharmacokinetics of the inhaled drug nemiralisib using an intravenous microtracer combined with an inhaled dose and an oral radiolabel dose in healthy male subjects. *Drug Metab Dispos* 47: 1457-1468.
- Hop CE, Wang Z, Chen Q, and Kwei G (1998) Plasma-pooling methods to increase throughput for in vivo pharmacokinetic screening. *J Pharm Sci* 87: 901-903.
- International Commission on Radiological Protection (1992) Radiological protection in biomedical research. ICRP Publication 62. *Ann ICRP* 22.
- International Conference on Harmonisation of Technical Requirements for Registration of Pharmaceuticals of Human Use (2009) Guidance on nonclinical safety studies for the conduct of human clinical trials and marketing authorization for pharmaceuticals M3(R2). https://database.ich.org/sites/default/files/M3_R2_Guideline.pdf. Accessed February 2, 2022.
- Johne A, Scheible H, Becker A, van Lier JJ, Wolna P, and Meyring M (2020) Open-label, single-center, phase I trial to investigate the mass balance and absolute bioavailability of the

- highly selective oral MET inhibitor tepotinib in healthy volunteers. *Invest New Drugs* 38: 1507-1519.
- Keck BD, Ognibene T, and Vogel JS (2010) Analytical validation of accelerator mass spectrometry for pharmaceutical development. *Bioanalysis* 2: 469-485.
- Lappin G (2016) Approaches to intravenous clinical pharmacokinetics: Recent developments with isotopic microtracers. *J Clin Pharmacol* 56: 11-23.
- Loi CM, Smith DA, and Dalvie D (2013) Which metabolites circulate? *Drug Metab Dispos* 41: 933-951.
- Pene Dumitrescu T, Joshi SR, Xu J, Zhan J, Johnson M, Butcher L, Zimmerman E, Webster L, Davidson AM, Lataillade M, and Min S (2021) A phase I evaluation of the pharmacokinetics and tolerability of the HIV-1 maturation inhibitor GSK3640254 and tenofovir alafenamide/emtricitabine in healthy participants. *Antimicrob Agents Chemother* 65: e02173-20.
- Penner N, Klunk LJ, and Prakash C (2009) Human radiolabeled mass balance studies: objectives, utilities and limitations. *Biopharm Drug Dispos* 30: 185-203.
- Podoll T, Pearson PG, Evarts J, Ingallinera T, Bibikova E, Sun H, Gohdes M, Cardinal K, Sanghvi M, and Slatter JG (2019) Bioavailability, biotransformation, and excretion of the covalent bruton tyrosine kinase inhibitor acalabrutinib in rats, dogs, and humans. *Drug Metab Dispos* 47: 145-154.
- Raje S, Callegari E, Sahasrabudhe V, Vaz A, Shi H, Fluhler E, Woolf EJ, Schildknecht K, Matschke K, Alvey C, Zhou S, Papadopoulos D, Fountaine R, Saur D, Terra SG, Stevens L, Gaunt D, and Cutler DL (2018) Novel application of the two-period microtracer approach to determine absolute oral bioavailability and fraction absorbed of ertugliflozin. *Clin Transl Sci* 11: 405-411.

- Roffey SJ, Obach RS, Gedge JI, and Smith DA (2007) What is the objective of the mass balance study? A retrospective analysis of data in animal and human excretion studies employing radiolabeled drugs. *Drug Metab Rev* 39: 17-43.
- Spinner CD, Felizarta F, Rizzardini G, Philibert P, Mitha E, Domingo P, Stephan CJ, DeGrosky M, Bainbridge V, Zhan J, Dumitrescu TP, Jeffrey JL, Xu J, Halliday F, Gan J, Johnson M, Gartland M, Joshi SR, and Lataillade M (2022) Phase IIa proof-of-concept evaluation of the antiviral efficacy, safety, tolerability, and pharmacokinetics of the next-generation maturation inhibitor GSK3640254. *Clin Infect Dis*. doi: 10.1093/cid/ciab1065.
- US Food and Drug Administration (2020) Safety testing of drug metabolites - guidance for industry. <https://www.fda.gov/media/72279/download>. Accessed February 2, 2022.
- Wang D, Lu W, and Li F (2015) Pharmacological intervention of HIV-1 maturation. *Acta Pharm Sin B* 5: 493-499.
- Wilson ID and Nicholson JK (2017) Gut microbiome interactions with drug metabolism, efficacy, and toxicity. *Transl Res* 179: 204-222.
- Young GC, Corless S, Felgate CC, and Colthup PV (2008) Comparison of a 250 kV single-stage accelerator mass spectrometer with a 5 MV tandem accelerator mass spectrometer--fitness for purpose in bioanalysis. *Rapid Commun Mass Spectrom* 22: 4035-4042.

FOOTNOTES

This study was funded by ViiV Healthcare.

Disclosures: BW, YZ, GCY, DK, AP, JP, JD, BJ, and JZ are employees of and may own stock in GSK. MJ is an employee of ViiV Healthcare and may own stock in GSK.

Reprint requests to:

Bo Wen

GSK R&D

1250 S Collegeville Rd

Collegeville, PA, 19426

Phone: 610-917-7000

E-mail: bo.1.wen@gsk.com

FIGURE LEGENDS

Figure 1. Study design. IV, intravenous. ^aIf radioactivity was >1% immediately before discharge, fecal samples were collected at home after Day 15.

Figure 2. Putative metabolic scheme for notable metabolites of GSK3640254 in human.

*indicates the position of the radiolabel incorporation.

Figure 3. Mean cumulative recovery of total radioactivity following administration of [¹⁴C]GSK3640254 as an **(A)** IV infusion and **(B)** oral suspension. IV, intravenous. ^an=3, with 2 additional participants with atypical recovery values not included.

Figure 4. Mean (SD) plasma concentrations of **(A)** parent GSK3640254 following oral tablet (2 × 100 mg) and IV infusion (100 µg) administration and **(B-C)** parent GSK3640254 vs total radioactivity following **(B)** IV infusion (100 µg) and **(C)** oral suspension (85 mg) administration. IV, intravenous.

Figure 5. Reconstructed AMS radiochromatograms of **(A)** pooled human AUC_{0-24h} plasma and **(B)** pooled human AUC_{0-96h} plasma following administration of 85 mg [¹⁴C]GSK3640254 as an oral suspension. AMS, accelerator mass spectrometry; AUC_{0-24h}, area under the concentration-time curve from time 0 to 24 hours; AUC_{0-96h}, area under the concentration-time curve from time 0 to 96 hours; DPM, disintegrations/minute.

Figure 6. Reconstructed AMS radiochromatograms of **(A)** pooled human feces and **(B)** pooled human duodenal bile following administration of 100 µg [¹⁴C]GSK3640254 as an intravenous infusion. AMS, accelerator mass spectrometry; DPM, disintegrations/minute.

Figure 7. (A) Reconstructed Topcount radiochromatograms of pooled human feces and **(B)** reconstructed AMS radiochromatograms of pooled human duodenal bile following oral administration of 85 mg [¹⁴C]GSK3640254. AMS, accelerator mass spectrometry; CPM, counts/minute; DPM, disintegrations/minute.

TABLES

Table 1. Summary of GSK3640254 Plasma PK Parameters

PK parameter	N	n	Route of administration	Geometric mean (%CVb) ^a
Derived from total radioactivity				
C _{max} , ng/mL	5	5	IV	7.46 (6.9)
	5	5	Oral	675 (13.6)
t _{max} , median (range), h	5	5	IV	0.983 (0.983-0.983)
	5	5	Oral	4.00 (1.50-6.00)
AUC _{0-t} , h·ng/mL	5	5	IV	102 (19.4)
	5	5	Oral	22,746 (20.4)
AUC _{0-∞} , h·ng/mL	5	5	IV	105 (19.1)
	5	5	Oral	23,227 (20.7)
t _{1/2} , h	5	5	IV	29.8 (11.3)
	5	5	Oral	30.1 (11.4)
CL, L/h	5	5	IV	1.03 (21.6)
CL/F, L/h	5	5	Oral	3.65 (20.7)
V _{ss} , L	5	5	IV	40.5 (28.3)
V/F, L	5	5	Oral	158 (20.6)

Oral tablet: GSK3640254 200 mg

C_{\max} , ng/mL	5	5	Oral	1293 (7.6)
t_{\max} , median (range), h	5	5	Oral	7.0 (4.5-9.0)
AUC_{0-t} , h·ng/mL	5	5	Oral	40,817 (14.2)
$AUC_{0-\infty}$, h·ng/mL	5	5	Oral	41,234 (14.5)
$t_{1/2}$, h	5	5	Oral	24.1 (16.4)
CL/F, L/h	5	5	Oral	4.85 (14.5)

IV infusion: [^{14}C]GSK3640254 100 μg

C_{\max} , ng/mL	5	5	IV	8.44 (12.0)
t_{\max} , median (range), h	5	5	IV	0.983 (0.983-0.983)
AUC_{0-t} , h·ng/mL	5	5	IV	93.3 (20.4)
$AUC_{0-\infty}$, h·ng/mL	5	5	IV	96.6 (19.7)
$t_{1/2}$, h	5	5	IV	21.7 (12.6)
CL, L/h	5	5	IV	1.04 (19.7)
$CL_{R,i}$, L/h	5	5	IV	0.0199 (29.2)
V_{ss} , L	5	5	IV	28.7 (21.9)

Oral suspension: [¹⁴C]GSK3640254 85 mg

C _{max} , ng/mL	5	5	Oral	628 (15.4)
t _{max} , median (range), h	5	5	Oral	4.0 (1.5-5.5)
AUC _{0-t} , h·ng/mL	5	5	Oral	18,828 (21.7)
AUC _{0-∞} , h·ng/mL	5	5	Oral	19,026 (21.8)
t _{1/2} , h	5	5	Oral	24.2 (5.1)
CL/F, L/h	5	5	Oral	4.47 (21.8)
CL _R /F, L/h ^b	5	5	Oral	0.0147 (30.1)

AUC_{0-∞}, area under the concentration-time curve from time 0 extrapolated to infinity; AUC_{0-t}, area under the concentration-time curve from time 0 to last quantifiable concentration; CL, clearance; CL_R/F, oral renal clearance; CL_{R,i}, renal clearance; CL/F, oral clearance; C_{max}, maximum observed concentration; CVb, between-participant coefficient of variation; IV, intravenous; PK, pharmacokinetic; t_{1/2}, terminal phase half-life; t_{max}, time of C_{max}; V, volume of distribution; V/F, oral volume of distribution; V_{ss}, volume of distribution at steady state.

^aExcept where noted for t_{max}. ^bCumulative amount of radioactivity in urine for treatment period 2 was used as a surrogate for GSK3640254 in urine to calculate CL_R/F.

Table 2. Absolute and Relative Bioavailability of Dose-Normalized GSK3640254

Dose-normalized PK parameter	Dose-normalized adjusted			
	geometric mean		Ratio (%CVw)	90% CI
Absolute bioavailability				
AUC _{0-∞} /dose, (h·ng/mL)/mg	Test (oral tablet)	206	0.214 (7.2)	0.194-0.235
	Reference (IV)	966		
AUC _{0-t} /dose, (h·ng/mL)/mg	Test (oral tablet)	204	0.219 (7.8)	0.198-0.243
	Reference (IV)	933		
Relative bioavailability				
AUC _{0-∞} /dose, (h·ng/mL)/mg	Test (oral suspension)	224	1.090 (8.2)	0.973-1.212
	Reference (oral tablet)	206		
AUC _{0-t} /dose, (h·ng/mL)/mg	Test (oral suspension)	222	1.090 (8.4)	0.969-1.216
	Reference (oral tablet)	204		
C _{max} /dose, (ng/mL)/mg	Test (oral suspension)	7.39	1.140 (12.1)	0.992-1.318
	Reference (oral tablet)	6.46		

AUC_{0-∞}, area under the concentration-time curve from time 0 extrapolated to infinity; AUC_{0-t}, area under the concentration-time curve from time 0 to last quantifiable concentration; C_{max}, maximum observed concentration; CVw, within-participant coefficient of variation; IV, intravenous; PK, pharmacokinetic.

Table 3. Summary of Plasma Metabolite Load, Hepatic Clearance, Hepatic Extraction, and Absorption Parameters

PK parameter	Treatment	N	n	Geometric mean	
				(%CVb)	95% CI
ML _{iv}	IV	5	5	0.0438 (363)	0.0058-0.3310
ML _{po}	Oral	5	5	0.180 (8.7)	0.162-0.201
CL _{h,iv,plasma} , L/h	IV	5	5	1.02 (20.0)	0.794-1.300
CL _{h,iv,blood} , L/h	IV	5	5	0.542 (20.0)	0.424-0.693
E _h	IV	5	5	0.00544 (20.0)	0.00426-0.00696
F _g	Oral	5	5	0.898 (5.5)	0.839-0.961
F _h	Oral	5	5	0.995 (0.1)	0.993-0.996
F _{abs}	Oral	5	5	0.260 (8.9)	0.232-0.290

CVb, between-participant coefficient of variation; CL_{h,iv,blood}, hepatic blood clearance; CL_{h,iv,plasma}, hepatic plasma clearance; E_h, hepatic extraction ratio; F_{abs}, fraction absorbed; F_g, fraction of drug escaping gut metabolism; F_h, fraction of drug escaping first-pass hepatic clearance; IV, intravenous; ML_{iv}, plasma metabolite load; ML_{po}, oral metabolite load; PK, pharmacokinetic.

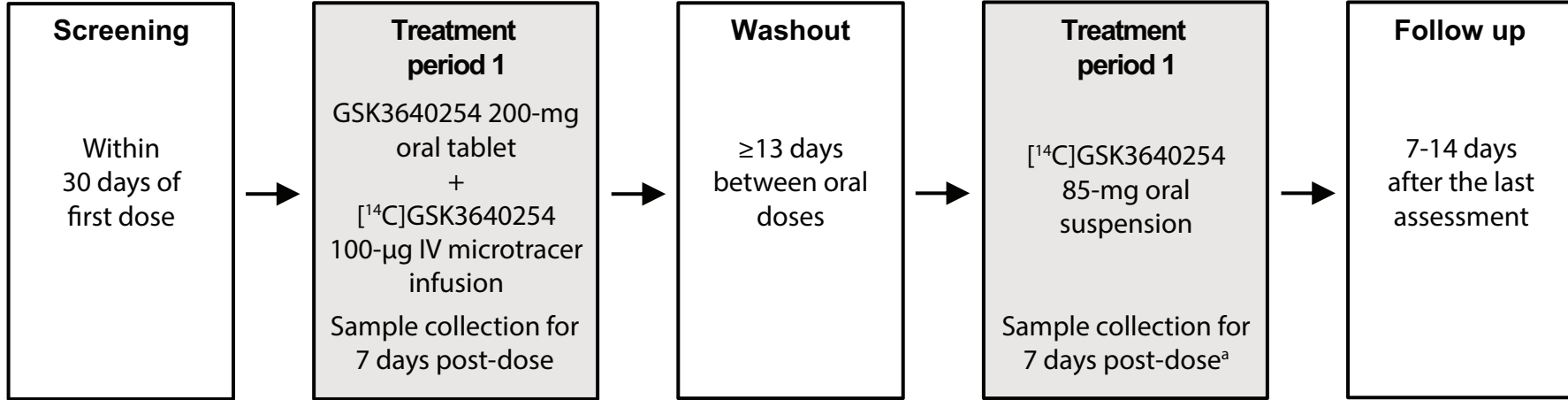


Figure 1

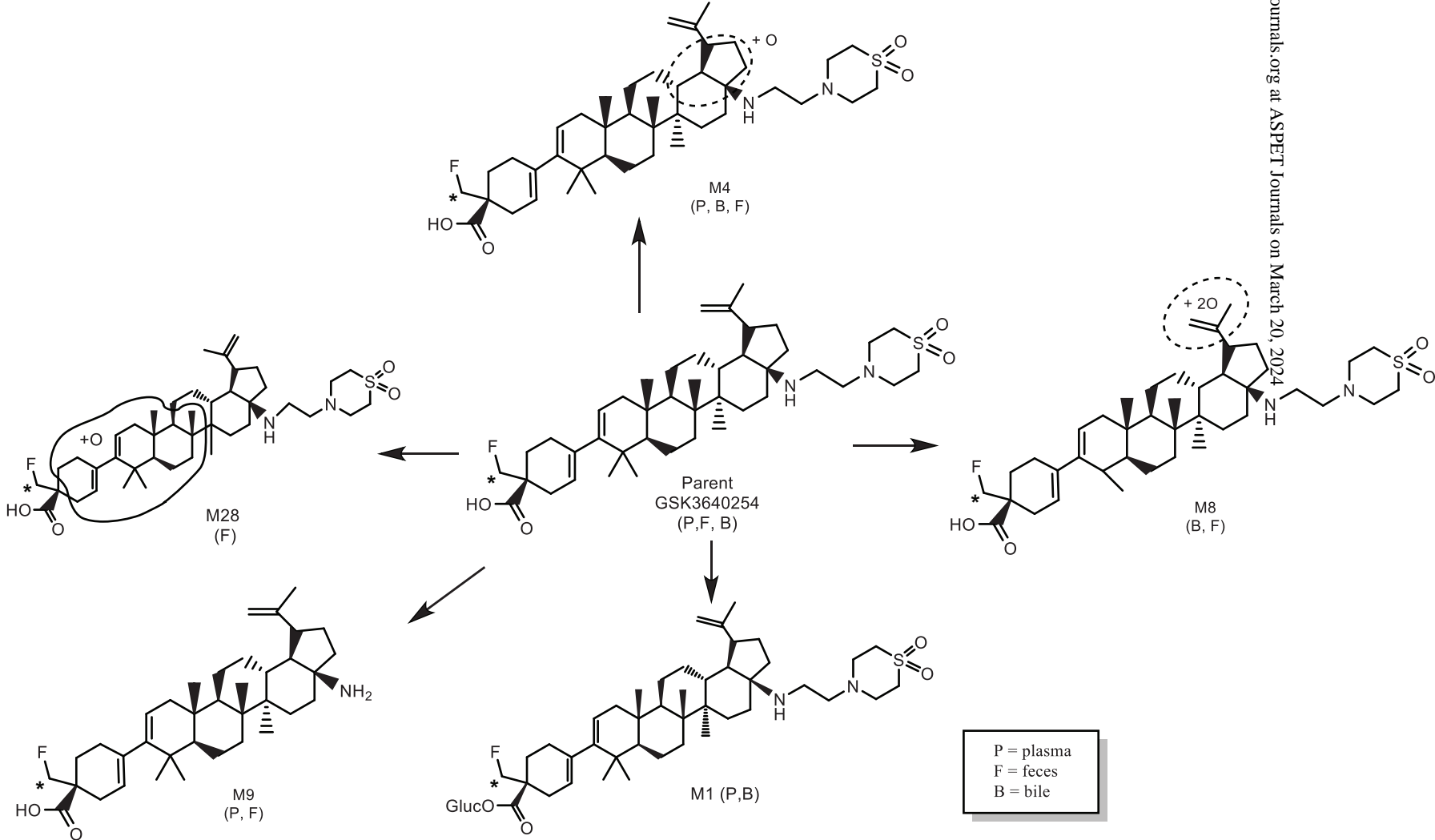
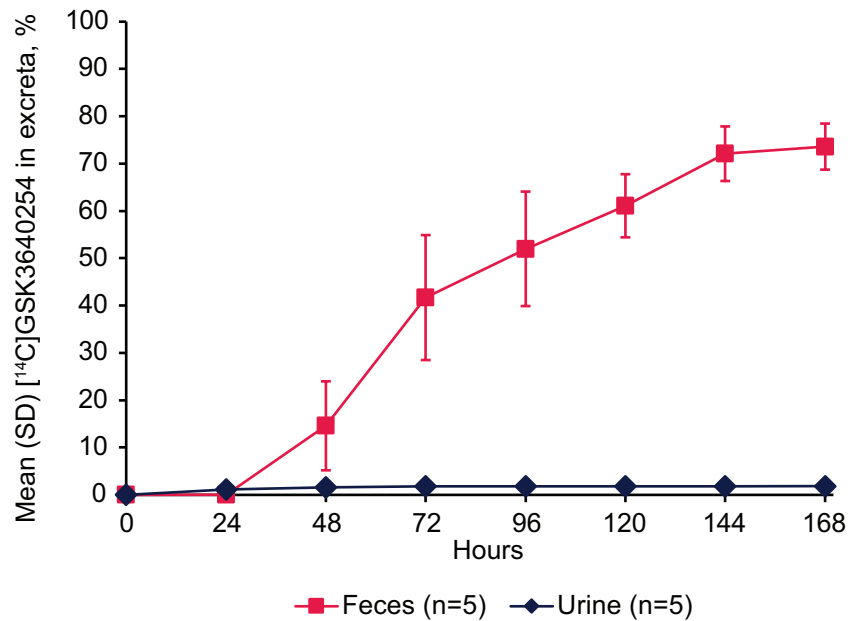
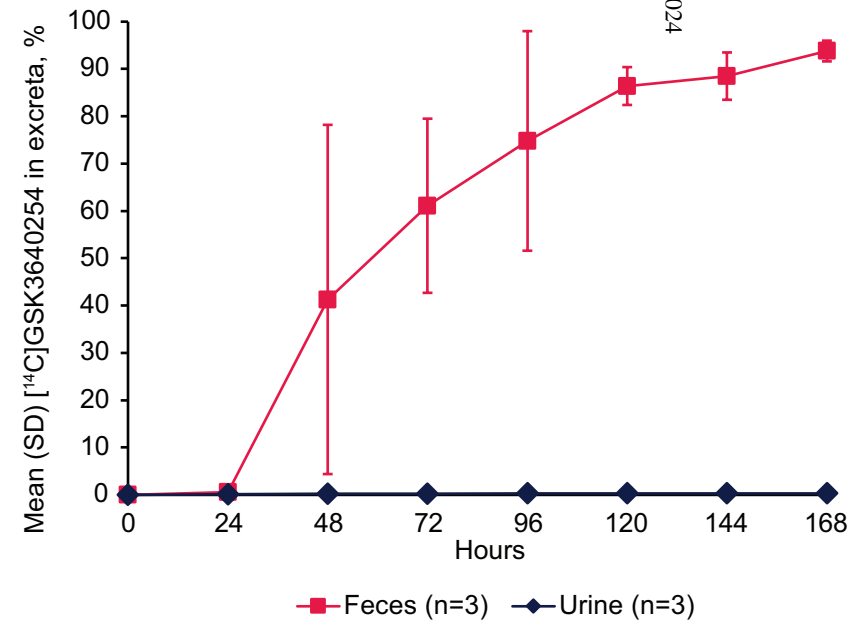


Figure 2

A**IV infusion (treatment period 1)****B****Oral suspension (treatment period 2)^a****Figure 3**

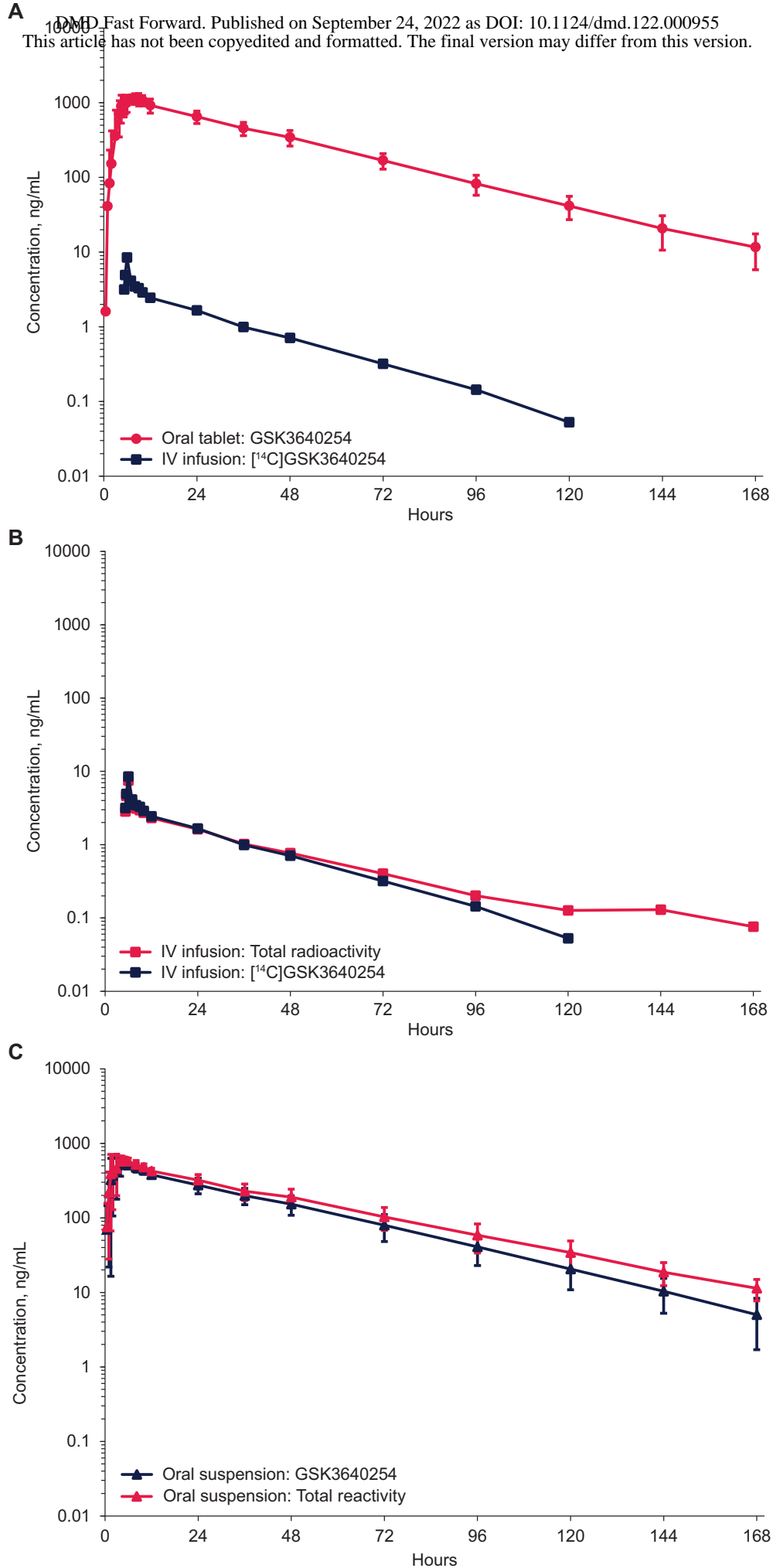


Figure 4

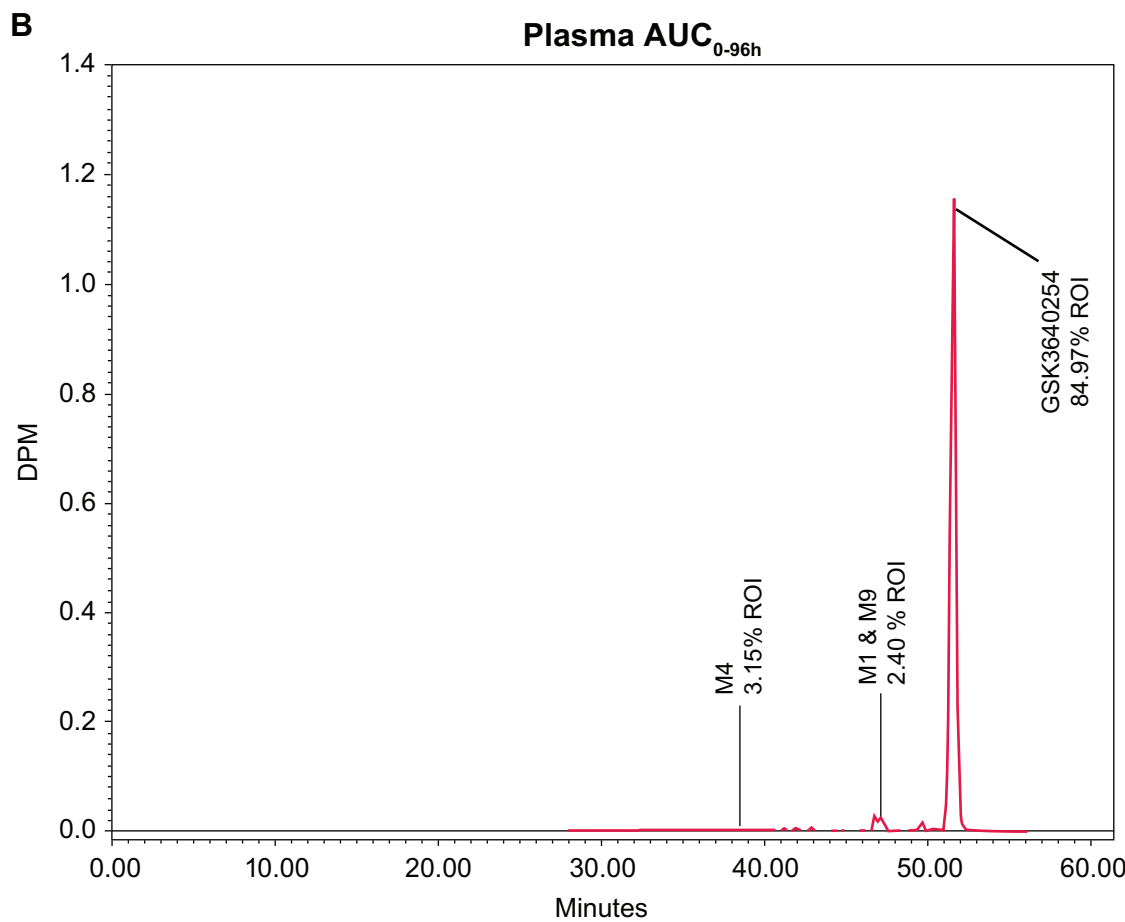
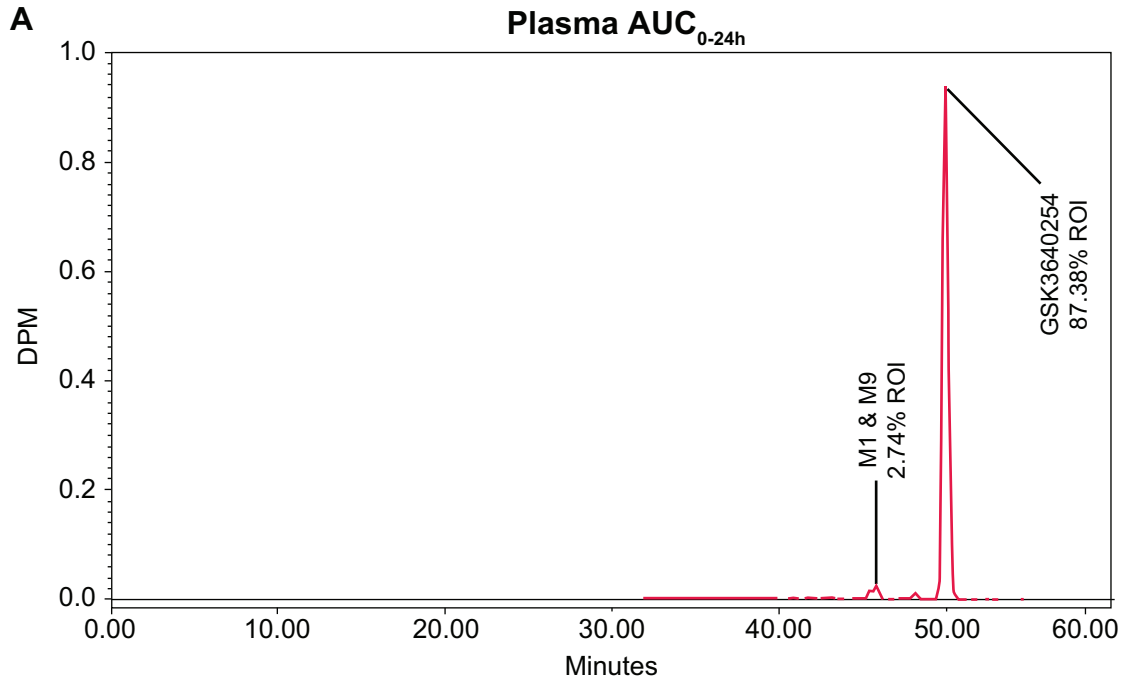


Figure 5

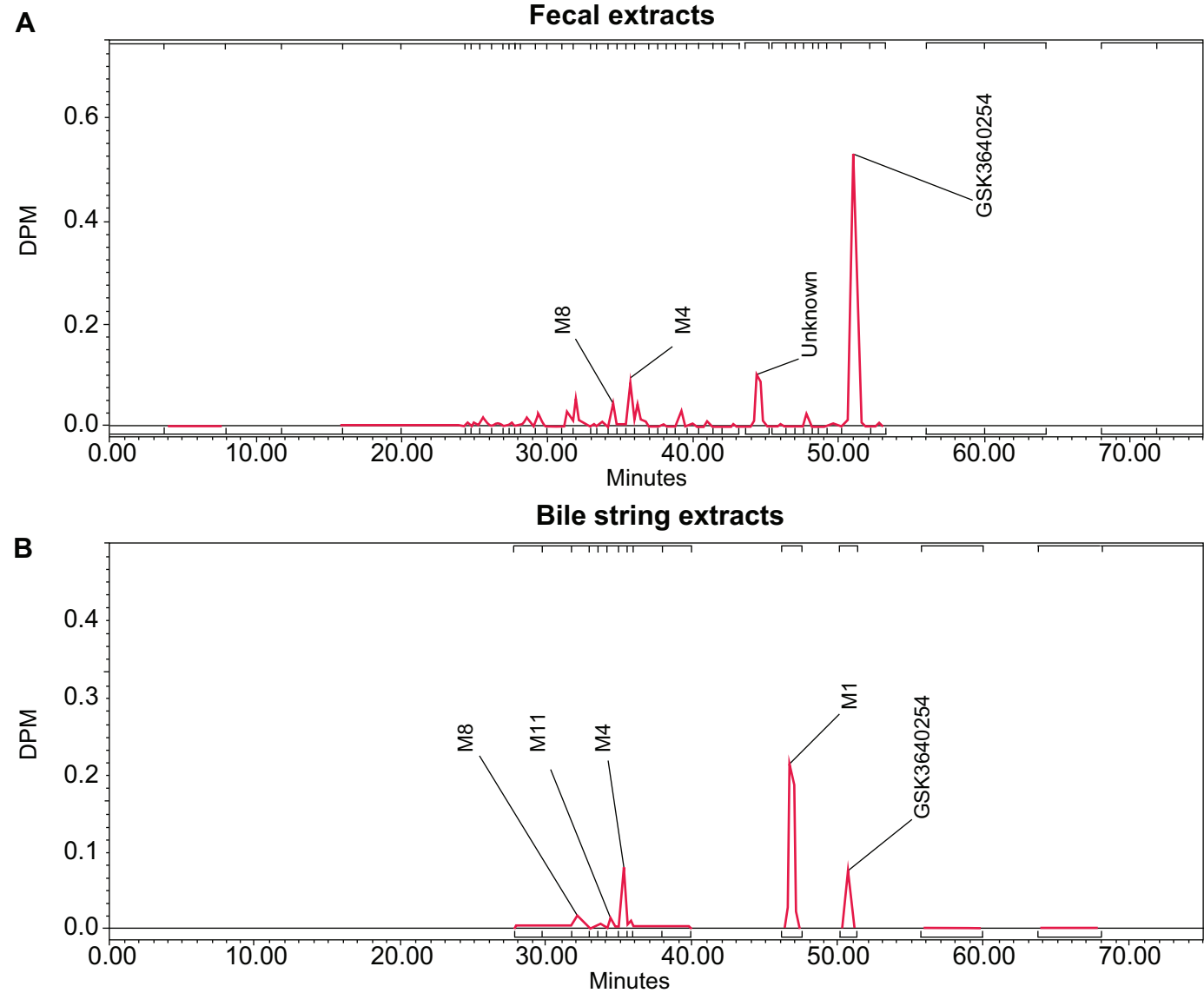


Figure 6

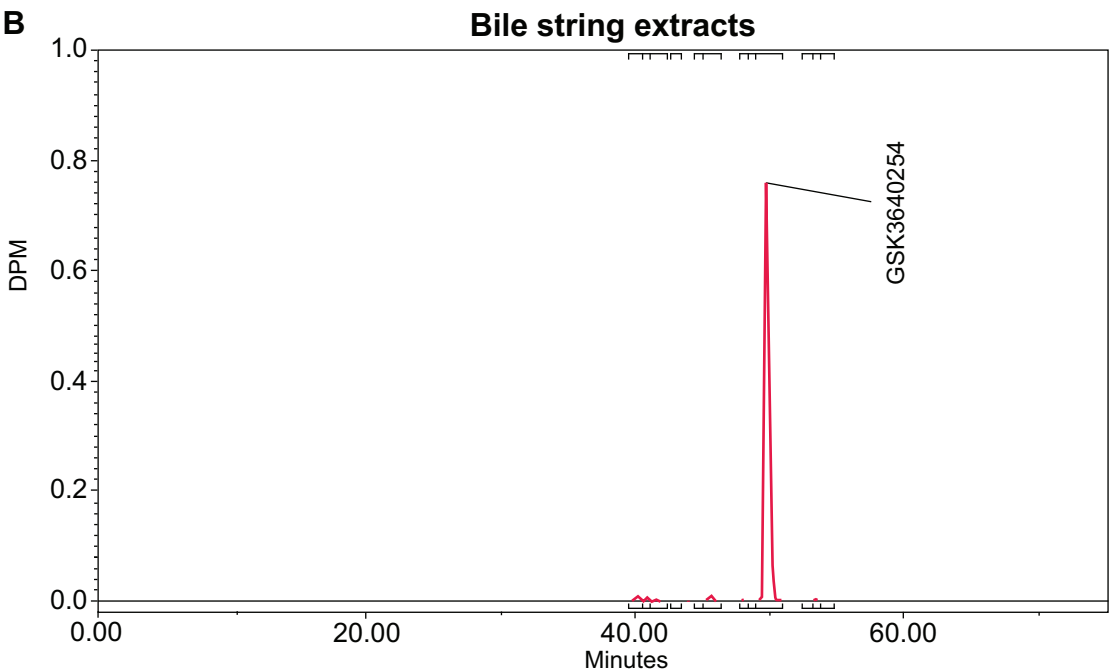
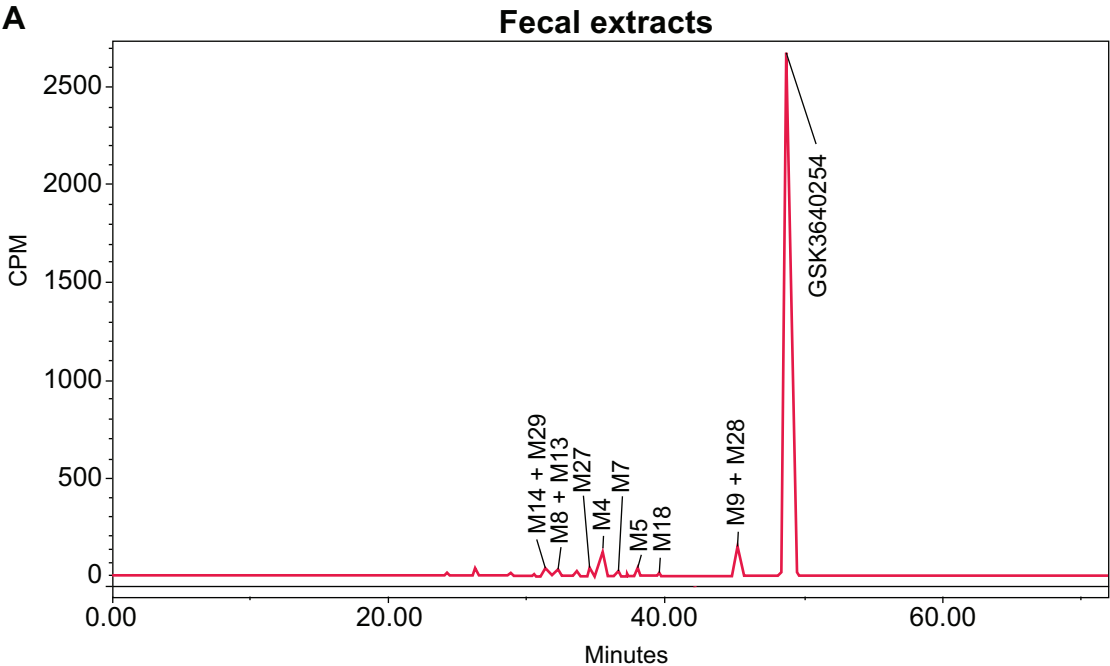


Figure 7

Manuscript Number: DMD-AR-2022-000955

SUPPLEMENTAL TABLE 1

**Investigation of Clinical Absorption, Distribution, Metabolism, and Excretion and
Pharmacokinetics of the HIV-1 Maturation Inhibitor GSK3640254 Using an Intravenous
Microtracer Combined With EnteroTracker for Biliary Sampling**

Bo Wen, Ying Zhang, Graeme C. Young, David Kenworthy, Adrian Pereira, Jill Pirhalla, Janine
Doyle, Bethany Jordon, Joyce Zhan, and Mark Johnson

*GSK, Collegeville, PA, USA (B.W., Y.Z, J.P., J.D., J.Z.) and GSK, Ware, UK (G.C.Y., D.K.) and
GSK, Stevenage, UK (A.P., B.J.) and ViiV Healthcare, Durham, NC, USA (M.J.)*

Journal: *Drug Metab Dispos*

Supplemental Table 1. Analytical Assays Used in Treatment Periods 1 and 2

Analysis	Period	Sample	Method or Assay
Mass balance and excretion	1	Urine	LSC or AMS
		Feces	LSC or AMS
	2	Urine	LSC
		Feces	LSC
PK	1	Plasma	LC-MS/MS for GSK3640254; LC + AMS for [¹⁴ C]GSK3640254; AMS for total radioactivity
	2	Plasma	LC-MS/MS for GSK3640254; AMS for total radioactivity
	1	Plasma	Not analyzed
		Feces	LC + AMS
Metabolic characterization	1	Bile	LC + AMS; LC-MS/MS
		Plasma	LC + AMS; LC-MS/MS
		Feces	HPLC-MS/MS
	2	Bile	LC + AMS; LC-MS/MS

AMS, accelerator mass spectrometry; HPLC, high-performance liquid chromatography; LC-MS/MS, liquid chromatography with tandem mass spectrometry; LSC, liquid scintillation counting; PK, pharmacokinetic.

Manuscript Number: DMD-AR-2022-000955

SUPPLEMENTAL TABLE 2

**Investigation of Clinical Absorption, Distribution, Metabolism, and Excretion and
Pharmacokinetics of the HIV-1 Maturation Inhibitor GSK3640254 Using an Intravenous
Microtracer Combined With EnteroTracker for Biliary Sampling**

Bo Wen, Ying Zhang, Graeme C. Young, David Kenworthy, Adrian Pereira, Jill Pirhalla, Janine
Doyle, Bethany Jordon, Joyce Zhan, and Mark Johnson

*GSK, Collegeville, PA, USA (B.W., Y.Z, J.P., J.D., J.Z.) and GSK, Ware, UK (G.C.Y., D.K.) and
GSK, Stevenage, UK (A.P., B.J.) and ViiV Healthcare, Durham, NC, USA (M.J.)*

Journal: *Drug Metab Dispos*

Supplemental Table 2. Summary of Participant Demographics

Demographic	Total^a (N=5)
Age, mean (SD), y ^b	37.4 (5.4)
Male, n (%)	5 (100)
Race, n (%)	
Central or South Asian Heritage	1 (20)
Black or African American	3 (60)
White or Caucasian/European Heritage	1 (20)
Ethnicity, n (%)	
Not Hispanic or Latino	5 (100)
Body mass index, mean (SD), kg/m ²	24.8 (3.3)
Height, mean (SD), cm	180.8 (4.8)
Weight, mean (SD), kg	80.7 (7.1)

SD, standard deviation.

^aAll participants were included in both treatment periods 1 and 2, therefore total is presented. ^bAge was imputed when full date of birth was not provided.

Manuscript Number: DMD-AR-2022-000955

SUPPLEMENTAL TABLE 3

**Investigation of Clinical Absorption, Distribution, Metabolism, and Excretion and
Pharmacokinetics of the HIV-1 Maturation Inhibitor GSK3640254 Using an Intravenous
Microtracer Combined With EnteroTracker for Biliary Sampling**

Bo Wen, Ying Zhang, Graeme C. Young, David Kenworthy, Adrian Pereira, Jill Pirhalla, Janine
Doyle, Bethany Jordon, Joyce Zhan, and Mark Johnson

*GSK, Collegeville, PA, USA (B.W., Y.Z, J.P., J.D., J.Z.) and GSK, Ware, UK (G.C.Y., D.K.) and
GSK, Stevenage, UK (A.P., B.J.) and ViiV Healthcare, Durham, NC, USA (M.J.)*

Journal: *Drug Metab Dispos*

Supplemental Table 3. Plasma Ratios of [¹⁴C]GSK3640254 (Treatment Period 1) and GSK3640254 (Treatment Period 2) to Total Radioactivity

PK parameter	Geometric mean (%CVb)	95% CI
Treatment period 1: Ratio of [¹⁴C]GSK3640254/total radioactivity^a		
C _{max} , (ng/mL)/(ngEq/mL)	1.13 (8.2)	1.02-1.25
AUC _{0-t} , (h·ng/mL)/(h·ngEq/mL)	0.917 (6.7)	0.844-0.996
AUC _{0-∞} , (h·ng/mL)/(h·ngEq/mL)	0.919 (6.3)	0.850-0.994
Treatment period 2: Ratio of GSK3640254/total radioactivity^b		
C _{max} , (ng/mL)/(ngEq/mL)	0.930 (4.2)	0.883-0.980
AUC _{0-t} , (h·ng/mL)/(h·ngEq/mL)	0.828 (2.3)	0.805-0.851
AUC _{0-∞} , (h·ng/mL)/(h·ngEq/mL)	0.819 (2.0)	0.799-0.840

AUC_{0-∞}, area under the concentration-time curve from time 0 extrapolated to infinity; AUC_{0-t}, area under the concentration-time curve from time 0 to last quantifiable concentration; C_{max}, maximum observed concentration; CVb, between-participant coefficient of variation; PK, pharmacokinetic.

^a[¹⁴C]GSK3640254 concentration was derived via liquid chromatography plus accelerator mass spectrometry. Total radioactivity was analyzed using accelerator mass spectrometry. ^bGSK3640254 concentration was derived via liquid chromatography with tandem mass spectrometry. Total radioactivity was analyzed using accelerator mass spectrometry.

Manuscript Number: DMD-AR-2022-000955

SUPPLEMENTAL TABLE 4

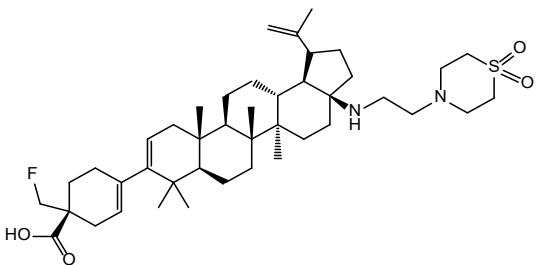
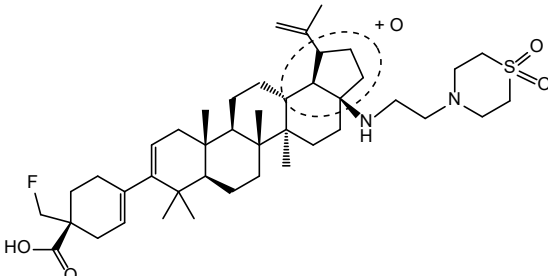
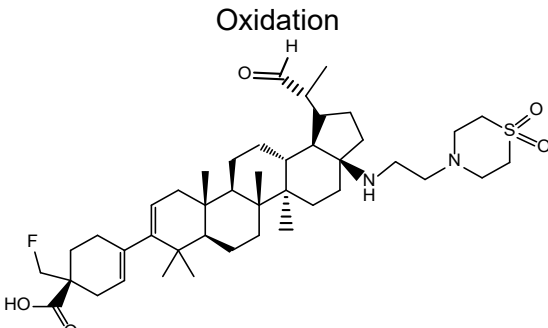
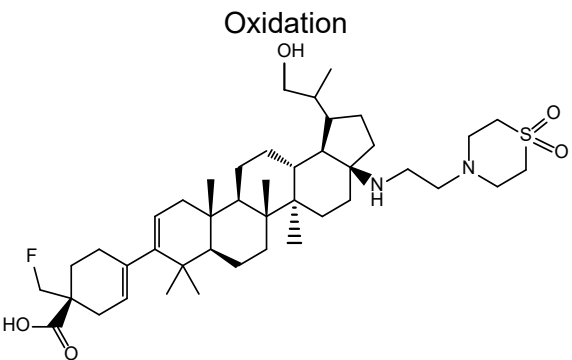
**Investigation of Clinical Absorption, Distribution, Metabolism, and Excretion and
Pharmacokinetics of the HIV-1 Maturation Inhibitor GSK3640254 Using an Intravenous
Microtracer Combined With EnteroTracker for Biliary Sampling**

Bo Wen, Ying Zhang, Graeme C. Young, David Kenworthy, Adrian Pereira, Jill Pirhalla, Janine
Doyle, Bethany Jordon, Joyce Zhan, and Mark Johnson

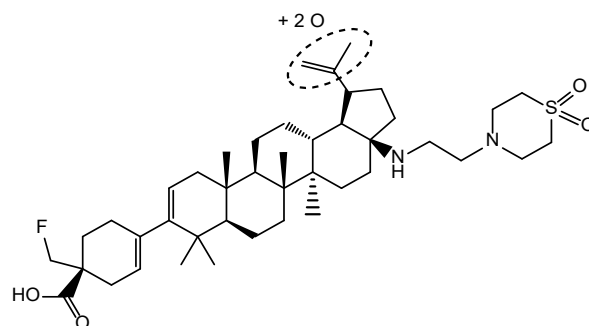
*GSK, Collegeville, PA, USA (B.W., Y.Z, J.P., J.D., J.Z.) and GSK, Ware, UK (G.C.Y., D.K.) and
GSK, Stevenage, UK (A.P., B.J.) and ViiV Healthcare, Durham, NC, USA (M.J.)*

Journal: *Drug Metab Dispos*

Supplemental Table 4. Metabolites Identified in Feces Following a Single Oral Administration of [¹⁴C]GSK3640254 to Human at a Target Dose Level of 85 mg (Treatment Period 2)

Peak ID	Metabolite structure	% matrix radioactivity (% dose)
P	 GSK3640254	84.3 (78.5)
M4		3.3 (3.1)
M5	 Oxidation	0.8 (0.8)
M7	 Hydration	0.5 (0.5)

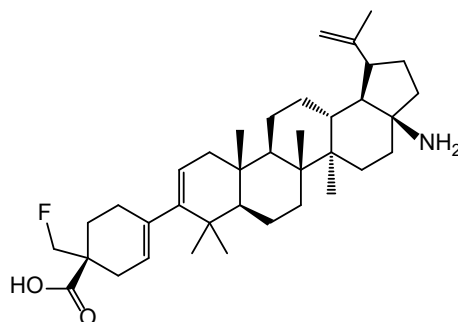
M8^a



1.0
(0.9)

Di-oxidation

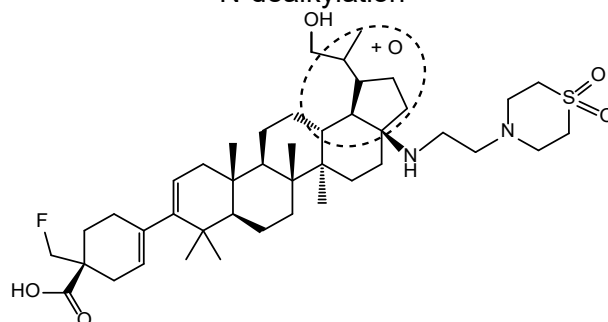
M9^b



5.3
(4.9)

N-dealkylation

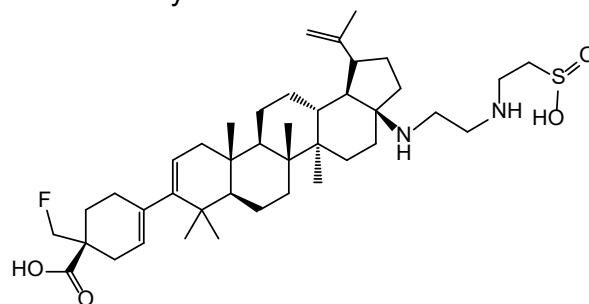
M13^a



1.0
(0.9)

Hydration and oxidation

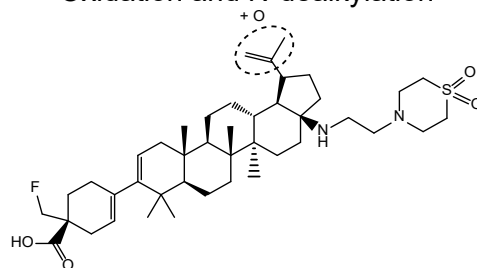
M14^c



1.1
(1.0)

Oxidation and N-dealkylation

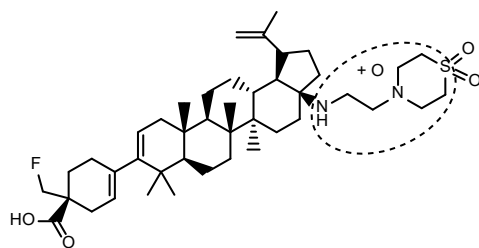
M18



0.3
(0.3)

Oxidation

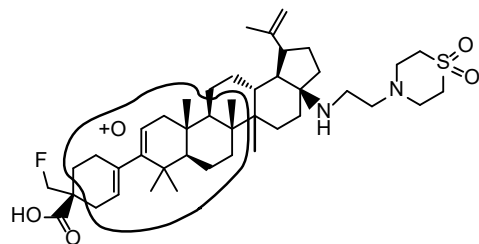
M27



1.1
(1.0)

Oxidation

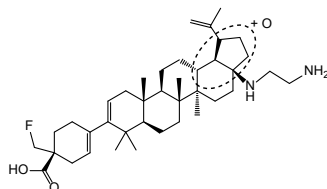
M28^b



5.3
(4.9)

Oxidation

M29^c



1.1
(1.0)

Oxidation and N-dealkylation

Total radioactive material assigned

97.7
(91.0)

% dose in matrix pool analyzed

93.1

Total % dose excreted in matrix

93.8

^aM8 co-eluted with M13. ^bM9 co-eluted with M28. ^cM14 co-eluted with M29.